THE ASTROPHYSICAL JOURNAL, 446:150–154, 1995 June 10

THE NATURE OF RADIO EMISSION IN QSO 1821+643, A RADIO-QUIET QUASAR WITH RADIO-LOUD PROPERTIES

PADELI P. PAPADOPOULOS,[1] E. R. SEAQUIST,[1] J. M. WROBEL,[2] AND L. BINETTE[3]
Received 1994 July 25; accepted 1994 December 20

ABSTRACT

We report principal results of a search for extended 6 cm continuum emission from 12 radio-quiet quasars using the Very Large Array (VLA). We report evidence for extended emission in QSO 1821+643 and tentative detection of similar structure in three others. We suspect that a low-radio power AGN resides in the center of the QSO 1821+643 host galaxy, ejecting plasma into a dust/gas-rich environment and creating extended ($\approx$76 kpc) low brightness radio emission. However, star formation may also be a contributor to the radio as well as to the far infrared (FIR) luminosity of this galaxy.

Subject headings: quasars: individual (QSO 1821+643) — radio continuum: galaxies

1. INTRODUCTION

During the past two decades, evidence has continued to mount that quasars and Seyfert galaxies are strongly related. More specifically, the observational evidence suggests that radio-quiet quasars (hereafter RQQs) are simply Seyfert 1 galaxies seen at a greater distance (Morgan & Dreiser 1983). Similar indications are found for the populations of radio-loud quasars (hereafter RLQs) in relation to the broad-line radio galaxies which, for the most part are E galaxies (Moffet 1975). The origin of FIR emission in both RQQs and Seyfert galaxies (Alloin et al. 1992; Barvainis 1990) appears to be thermal emission from a mixture of hot and cool dust (Edelson et al. 1987; Telesco 1992). However, nonthermal FIR emission is suspected in some Seyfert 1 and unreddened quasars (e.g., Edelson & Malkan 1986) and the issue remains contentious.

The morphology of any extended radio component and the relation of its luminosity to the FIR luminosity, can give clues about its origin and whether star formation or an AGN plays the dominant role in activating these objects. Radio emission with collimated jet morphology is a good signature of the dominant presence of an AGN at these wavelengths. On the other hand, the tight correlation between the FIR and radio luminosities (van der Kruit 1973; Helou, Soifer, & Rowan-Robinson 1985) indicates that star formation is a key factor. Any deviation from this relation may indicate that some process other than star formation provides the energy input. However, deviation from the FIR/radio correlation alone cannot demonstrate the existence of significant contribution from an AGN. More evidence is (e.g., presence of jets, parsec scale components, variability) is needed.

This study presents a search for extended radio emission from 12 infrared-bright RQQs for which radio and/or infrared measurements strongly suggest the presence of the host galaxy. The purpose is to examine the structure of the extended emission with the view to identify its origin in the context of the above discussion. Throughout this study we assume $H_0 = 75$ km s^{-1} Mpc^{-1} and $q_0 = 0.5$.

2. SELECTION CRITERIA

We selected 12 radio quiet quasars ($M_B < -23$) from a larger VLA[4] survey by Kellerman et al. (1989) and from an *IRAS* catalog of quasars by Neugebauer et al. (1986). Our operational definition of radio quiet is that the radio power at 6 cm is $P_{6\,\mathrm{cm}} \leq 10^{24}$ W Hz^{-1}. An alternative definition of a radio-quiet quasar uses the ratio R of the radio to the optical fluxes (Kellerman et al. 1989). According to this determination, a RQQ has a value of $R \leq 10$. Use of this parameter would not change our sample significantly. The value of R for 11 quasars in our sample is $R < 10$, except for Mrk 231 for which $R = 25$. We selected quasars with strong FIR emission since they should have significant contribution from warm dust, heated by star-forming regions and/or an AGN and hence are likely to exhibit extended radio continuum. For the same purpose we selected quasars that have the lowest value for f_c, where f_c is the ratio of the core flux measured by the A configuration at 0.″5 resolution to the total flux (or the flux of a more extended component) measured by the D configuration at 15″ resolution (Kellermann et al. 1989). In some cases we selected particularly promising candidates that are contained in only one catalog, and in these cases we have used only one of the above selection criteria.

3. OBSERVATIONS AND DATA REDUCTION

Our observations were conducted with the VLA in B configuration at 6 cm using four 50 MHz IF channels recording the LHC and RHC polarizations. In order to optimize the *u-v* plane coverage the observing time for each object was divided into 3 × 15 minute intervals, widely separated in hour angle. We observed a phase calibrator every 15 minutes. Absolute flux density calibration was achieved using the standard sources 3C 286 and 3C 48. The angular resolution of our observations was typically 1.″5–2.″5 and the rms noise in our naturally weighted maps is 30–35 μJy beam, which is similar to the theoretical noise level except in one case where the noise is around 90–100 μJy beam^{-1} due to a nearby strong source.

We employed phase self-calibration in eight of our sources in order to reduce the effect of atmospheric (Schwab 1980) errors. In four cases (0710+457, 1211+143, 1440+356,

[1] Department of Astronomy, University of Toronto, St George 60 Street, Toronto, Canada M5S 1A7.
[2] National Radio Astronomy Observatory, P.O. Box 0, Socorro, NM 87801.
[3] Space Telescope Science Institute, 3700 San Martin Drive, Baltimore MD 31218.

[4] The VLA is a facility of National Radio Astronomy Observatory, operated by Associated Universities, Inc., under cooperative agreement with the National Science Foundation.

1216−015) the field of view contained strong sources (>90 mJy) that allowed us to employ self-calibration effectively even though the program sources are weak. The fields of 0157+001, 1700+518, 1254+571, and 1821+643 had no strong background sources, but the program sources themselves had peak flux densities of $S \geq 5.5$ mJy in naturally weighted maps, and were strong enough to apply phase self-calibration. In order to ensure that self-calibration worked properly for all our sources we used two to three different models per source to check whether self-calibration converged to the same brightness distribution for all models. This was found to be the case for the eight objects for which we have applied the method. We then made maps for all eight sources using the AIPS task "MX."

In the cases where no extended emission was clearly apparent in the source map the visibility data were modeled directly in order to extract structural information on its brightness distribution. The reason for this approach is that it avoids the intermediate step of mapping and deconvolution, a process which is nonlinear and which we found to have some unpredictable results for sources with weak extended emission. Modeling the u-v data avoids uncertainties introduced by this step. The uncertainties are particularly severe when the faint extended component is comparable in size to the synthesized beam and therefore cannot be resolved in the image plane.

The procedure used was to first shift the source position to the phase center of the image and to remove all other sources from the field of view. We then assume that the source structure can be well described by a point source component with flux density S_p and a circular Gaussian halo of FWHM θ and total flux density of S_h. The brightness distribution then can be expressed as follows:

$$B(\xi, n) = (2\pi\theta^2)^{-1} S_h e^{-(\xi^2+n^2)/2\theta^2} + S_p \delta(\xi, n)\,, \qquad (1)$$

where (ξ, n) are spatial coordinates in the sky. The information provided directly by an interferometer are the values of visibilities $V(u, v)$ which are the Fourier transform coefficients of the source brightness distribution. For the assumed brightness distribution the real part of the visibility is given by

$$ReV(u, v) = S_p + S_h e^{-2\pi^2\theta^2(u^2+v^2)}\,, \qquad (2)$$

and since the function describing the source brightness is even, the imaginary part of the visibility will be

$$\text{Im } V(u, v) = 0 \qquad (3)$$

where (u, v) are the coordinates of the projected (onto the sky) interferometer baselines. We have used equation (2) to obtain a least-square fit of the real part of our visibility data after azimuthal averaging to improve the S/N. This yielded an estimate of θ, S_p, and the total flux density $S_t = S_p + S_h$ for three sources (0157+001, 1254+571, 1700+518) where the model gave a good fit to the visibility data. For the same sources we found that Im $V(u, v) \approx 0$ up to the longest baselines used for our fit, as expected from equation (3).

4. RESULTS

Of the 12 RQQs observed we detected 11 above the 5 σ level. Extended emission was successfully mapped only in the case of QSO 1821+643, but examination of the visibility data as described above indicates the presence of extended emission in three other cases. The characteristics of the observed objects are summarized in Table 1.

The RQQs with extended radio emission are 0157+001 (Mrk 1040), 1254+571 (Mrk 231), 1700+518, and 1821+643. Only 1821+643 clearly shows extended, low-brightness radio emission in the image plane, while the other three show signs of extended emission only in the visibility plane. In Figure 1 we have plotted the FIR luminosity (as defined by Helou et al. 1985) versus the radio power at 6 cm for ordinary, star forming galaxies from Wunderlich, Klein, & Wielebinski (1987) together with the four objects with detected extended radio

TABLE 1

CHARACTERISTICS OF OBSERVED OBJECTS

Name (1)	z (2)	θ (3)	D (4)	$S_p(\sigma)$ (5)	$S_t(\sigma)$ (6)	f_c (7)	Morphology (8)
0157+001.....	0.164	1.″0	2.4	3.71 (0.30)	8.80 (0.30)	0.42	CE
0710+457.....	0.056	≤3.5	≤3.4	1.60 (0.06)	1.70 (0.10)	0.94	Unresolved
0804+761.....	0.100	≤2.0	≤3.2	0.80 (0.04)	0.90 (0.10)	0.88	Unresolved
1211+143.....	0.085	≤2.3	≤3.2	1.00 (0.07)	0.80 (0.20)	1.25	Unresolved
1216−015.....	0.041	...	...	≤0.20	...	...	...
1254+571.....	0.041	1.1	0.8	246.0 (7.40)	252.0 (7.60)	0.97	CE
1402+261.....	0.164	≤2.5	≤6.0	0.50 (0.03)	0.51 (0.09)	1.00	Unresolved
1440+356.....	0.077	≤2.3	≤3.0	1.40 (0.05)	1.40 (0.10)	1.00	Unresolved
1449+588.....	0.210	≤2.5	≤7.2	0.35 (0.03)	0.60 (0.10)	0.58	Unresolved
1613+658.....	0.129	≤1.6	≤3.2	1.70 (0.06)	2.00 (0.10)	0.85	Unresolved
1700+518.....	0.292	1.6	5.7	3.14 (0.20)	8.13 (0.40)	0.38	CE
1821+643.....	0.296	21	76	11.24 (0.35)	19.50 (0.60)	0.57	Extended

NOTES.—Col. (1): Source name. Col. (2): Redshift. Col. (3): Angular size (in arcseconds). Col. (4): Proper length (in kiloparsecs) corresponding to the quoted angular diameter and the redshift of the object. Col. (5): Upper limit of the flux density (in millijanskys) of the unresolved component and the value of the rms noise σ. The value of this limit is estimated from the peak brightness (millijansky per beam) in uniform weighted maps (beam ≈1.″5), except in the three cases where the limit is obtained from the fitting process of the associated visibility data. Col. (6): Total integrated flux density (in millijanskys) within a box 40″ × 40″ around the source in a tapered, naturally weighted map (the applied tapering gives a beam ≈5″) and the value of the rms noise σ. Col. (7): Ratio of flux density of the unresolved component to the total flux density. Col. (8): Morphology; CE = core + extended emission, deduced from the fitting of the visibility data.

The noise is $\sigma = (\sigma_{cal}^2 + \sigma_{noise}^2)^{1/2}$, where $\sigma_{cal} = 0.03S$ (S is the measured flux density) is the 3% error in linking to the Baars et al. 1977 flux density scale. In col. (5) σ_{noise} is the rms noise in the map, and in col. (6) it is $\sigma_{noise} = N^{1/2}\sigma_{rms}$, where $N \approx 64$ is the number of beam areas (HPBW = 5″) contained within the 40″ × 40″ region centered on our source and σ_{rms} is the rms noise in the tapered map. In the cases where the visibility data were used σ_{noise} is obtained from the fitting process.

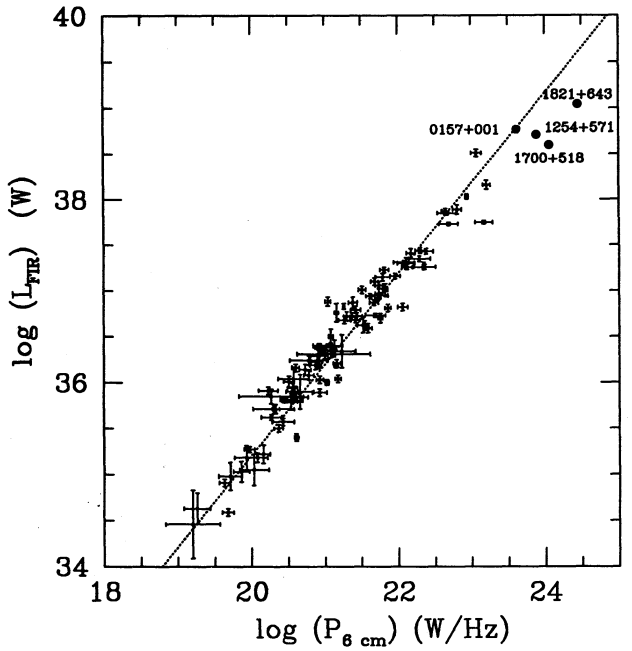

FIG. 1.—Far-infrared luminosity vs. radio power diagram ($\lambda = 6$ cm). The line indicates the least-squares fit of the correlation. The dispersion is $\sigma = 0.25$ along the $P_{6\,cm}$ axis. four of our *IRAS* bright RQQs are shown in the upper right marked with filled circles. Their associated errors are $\delta(\log L_{FIR}) \approx 0.02$–$0.07$ and $\delta(P_{6\,cm}) \approx 0.01$–$0.02$.

emission. The line represents a least-squares fit (with errors considered only in measured radio power since they are the most significant). The resulting dispersion is $\sigma = 0.25$ in log $P_{6\,cm}$, and it is indicative of the tightness of the FIR-radio correlation which is thought to arise in galaxies which derive most of their radio and FIR luminosity from star formation. From this diagram we can see that three of the RQQs (1254+571, 1700+518, 1821+643) deviate from this correlation by emitting more than the expected radio power. This can be considered as one of the manifestations of an AGN present in these objects (Condon & Broderick 1988; Wrobel & Heeschen 1988). In the case of 1254+571 (Mrk 231) the deviation is rather marginal ($\approx 2\ \sigma$). Nevertheless, it is interesting to note that high-resolution VLBI observations (Preuss & Fosbury 1983) have revealed significant emission [log $P_{6\,cm}$ (VLBI) = 23.4 W Hz^{-1}] coming from a central region $<0''.001$ (1 pc) in extent. This shows that, in this case, the AGN contributes a significant ($\approx 30\%$) part of the total radio power observed, and it may be responsible for the deviation from the FIR-radio correlation. In the other two cases (1821+643, 1700+518) the deviations from the correlation are somewhat larger ($\approx 4\ \sigma$) suggesting that the AGN may contribute a significant part of the radio power. However, previous high-resolution observations at 6 cm (Hutchings, Neff, & Gower 1992; Hutchings & Neff 1991) of these two objects detect some emission from unresolved components only in the case of 1700+518 but not in the case of 1821+643. This could be due to extended radio emission from the AGN (jets, lobes?) but it is unlikely in the case of 1821+643 since our maps of the extended radio emission show no clear-cut AGN characteristics (i.e. collimated jets, lobes). Therefore the deviation from the FIR-radio correlation remains the sole evidence for a significant AGN contribution to the emitted radio power and further evidence will be needed for a firm conclusion. We address the nature of the radio emission in QSO 1821+643 in more detail in the next section.

5. QSO 1821+643

Here we elaborate on this very rare example of an optically luminous quasar ($M_B \approx -27$), a RQQ that seems to have many of the characteristics associated with RLQs. Indeed, Ellingson, Yee, & Green (1991) present a persuasive case that optically luminous ($M_B \approx -27$) quasars are usually found in rich clusters only at high redshift ($z > 0.5$) and then only when they are radio loud, QSO 1821+643 seems to counter both these trends. In addition it lies at the center of a giant elliptical galaxy (Hutchings & Neff 1991) which is considered a "classic" host galaxy of RLQs. Moreover, it has a high nuclear accretion rate $\approx 19\ M_\odot\ \mathrm{yr}^{-1}$ (Kolman et al. 1991) which would be expected to occur more often (even though not exclusively) in RLQs.

In Figure 2 our radio map reveals extended ($21'' \approx 76$ kpc) low brightness ($S \approx 0.20$ mJy beam^{-1}) emission associated with 1821+643, the cross marks the optical position of the QSO (Kolman et al. 1991) and the extend of the host galaxy reported by Hutchings & Neff (1991) is shown by a circle. The optical observations show an almost spherical host galaxy with a radius of $\approx 12''$ (44 kpc) and with no structure even at a resolution of $0''.4$ (Hutchings & Neff 1991). These properties are not expected in terms of the simple unification scheme that considers RQQs as Seyfert 1 galaxies (usually spirals) at higher redshifts.

This QSO is quite red according to broadband colors $B-R = 1.1$ and $V-I = 1.3$ (Hutchings & Neff 1991) (even though the better sampled spectrum by Kolman et al. (1991) indicates a turnover only shortward of 2000 Å) it is the most luminous FIR emitter in our sample ($L_{FIR} \approx 6 \times 10^{12} L_\odot$). Recent observations of the sub-millimeter continuum (Hughes et al. 1993), as well as the red (for a QSO) colors of the nucleus, suggest the presence of heated dust, but the possibility of sig-

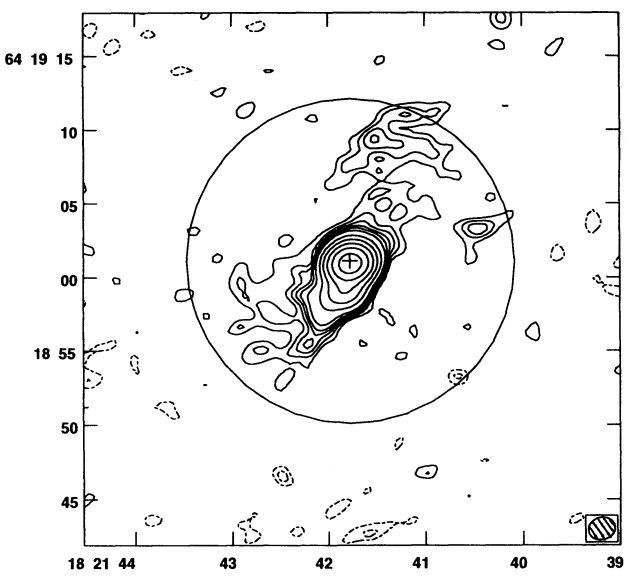

FIG. 2.—Naturally weighted contour map of the low brightness, extended radio emission at 6 cm (B-array) together with the optical position of QSO 1821+643 and a circle indicating the extent of the spherical host galaxy. The contours are $(-4, -3, -2, -1.5, -1, 1, 1.5, 2, 2.5, 3, 4, 8, 16, 32, 64, 128, 256, 512) \times 60\ \mu$Jy beam^{-1}. The rms noise is 30 μJy beam^{-1} and the restoring beam is also shown. The coordinate system used is B1950.

nificant contribution from a synchrotron power law cannot be ruled out (Kolman et al. 1991). The estimated dust mass is $M_d \approx 10^9 M_\odot$ ($\epsilon_\lambda \propto \lambda^{-1}$). Observations of CO so far yield only an upper limit (Alloin et al. 1992) but this upper limit is comparable to the CO flux expected for the observed dust mass (Alloin et al. 1992). If subsequent observations fail to detect CO at a level of ≈ 0.2 of the present upper limit it would suggest that part of the FIR flux density (used to estimate the dust mass) is of nonthermal origin.

As noted in the previous section (§ 4) our integrated radio flux density gives $\log P_{6\,\mathrm{cm}} = 24.45 \pm 0.01$ W Hz^{-1} which deviates (at a 4 σ level) from the FIR-radio correlation suggesting a significant contribution of the AGN in the observed radio power. This AGN is possibly associated with the peak brightness located within 0".5 of the optical position given by Kolman et al. (1991). However, previous A configuration observations (Lacy, Rawlings, & Hill 1992; Hutchings & Neff 1991) failed to detect any compact nuclear component, with a reported upper limit of 0.3 mJy ($P_{6\,\mathrm{cm}} < 10^{23}$ W Hz^{-1}), but they did detect extended central radio emission and a barely resolved southern knot linked to the central emission by a bent linear structure 2" in extent. The total flux associated with this emission (at 6 cm) is ≈ 13 mJy and it has a maximum angular extent of 4" (≈ 14 kpc). Our untapered uniformly weighted (Fig. 3) B configuration map (resolution $\approx 1".4$) shows a similar central linear structure aligned with the faint knot observed in the A configuration and with approximately the same angular size. This linear morphology suggests that the emission in the central 2"–4" is influenced by an AGN. In addition the 60 and 25 μm fluxes indicate dust warmer (75 K) than that inferred from the 60 and 100 μm bands (34 K). This is frequently observed in galaxies that show AGN activity even though there is a significant overlap with starbursts (de Grijp, Miley, & Lub 1987).

However, the view of the AGN as the main contributor to the observed radio emission of 1821+643 has to answer two basic questions, namely (1) Why the large-scale radio emission seen in our map (Fig. 2) does not show clear signs of AGN origin, i.e., highly collimated jets and lobes? (2) If the small-scale linear structure "seen" with the A-array (Lacy et al. 1992; Hutchings & Neff 1992), and shown at a lower resolution in Figure 3, is indeed a jet, then where is the associated core?

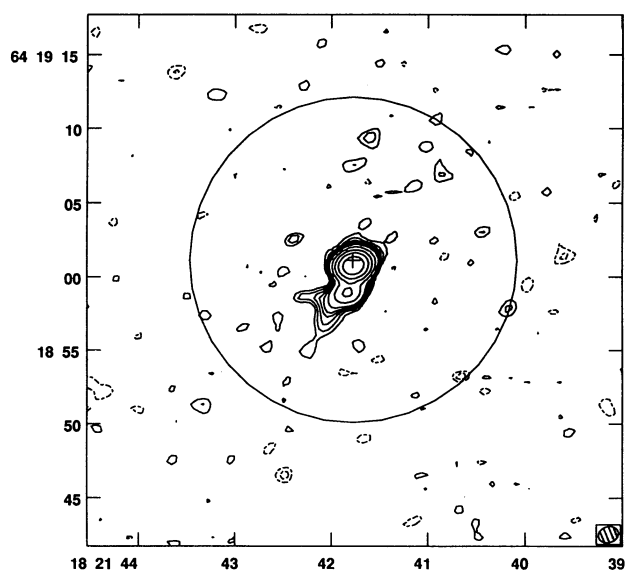

FIG. 3.—Uniformly weighted contour map of the radio emission at 6 cm (B-array) together with the optical position of QSO 1821+643 and a circle indicating the extent of the spherical host galaxy. The contours are (−4, −3, −2, −1.5, −1, 1, 1.5, 2, 2.5, 3, 4, 8, 16, 32, 64, 128, 256, 512) × 90 μJy beam^{-1}. The rms noise is 45 μJy beam^{-1} and the restoring beam is also shown. The coordinate system used is B1950.

A possible answer to the first question is that the presence of large amounts of dust/gas can suppress the growth of jets very effectively since neutral particles can be entrained by the jet stream very effectively causing the onset of turbulence and leading to large opening angles and diffusion of the jet (Hutchings & Neff 1991; Kundt 1987). This may be the reason why this QSO does not show any collimated, large-scale radio emission, often associated with radio-loud quasars. The large estimated dust mass, as well as the red colors of the nucleus suggest that there is a large reservoir of dust/gas present in 1821+643, and it is important to confirm the presence of the gas directly using CO observations. If CO is detected then the next important step is to obtain information about the location of the molecular gas with respect to the nucleus.

A possible answer to the second question is that there is a lack of significant radio emission from a compact core because of its small size. More specifically, if one considers the region close to the AGN's accretion disk as the one where electrons are accelerated at relativistic energies emitting synchrotron self-absorbed radiation (Blandford & Rees 1991) then one way of explaining the lack of significant radio emission from this region is because its size is rather small (and so will be the core flux density associated with it) due to a small accreting region. There is some observational evidence for the presence of a small accretion disk from the results of Kolman et al. (1991). They fitted the overall continuum spectrum of 1821+643 with a power law and a superposed geometrically thin, optically thick accretion disk spectrum. They maintain that the only way to explain the narrow UV bump observed (assumed to arise from the accretion disk) is to invoke a small disk size $R_{\mathrm{out}} \approx 12 R_{\mathrm{in}}$, where $R_{\mathrm{in}} = 3R_{\mathrm{Sch}}$ is the innermost stable orbit, (Shakura & Sunyev 1973). The size of the accretion disk can therefore be approximated by $R_{\mathrm{out}} \approx 36\ GM\ c^{-2}$, where M is the mass of the central accreting object. From Kolman et al. $M \approx 3 \times 10^9\ M_\odot$, thus $R_{\mathrm{out}} \approx 5 \times 10^{-3}$ pc and the corresponding angular size it would be $\theta \approx 10^{-6}$ arcsec. If we consider this angular size as a lower limit of the true size of the region emitting synchrotron self-absorbed radiation at a brightness temperature $T_b = 10^{12}$ K (the limit set by the inverse Compton effect) we estimate a compact core flux density of $S_{\mathrm{core}} \geq 0.02$ mJy. However, it is very likely that the compact region responsible for the synchrotron self-absorbed emission is much larger than the size of the accretion disk itself (Marscher 1991) and in such a case the associated flux density will be higher. For example, for a region just 3 times the estimated size of the accretion disk $S_{\mathrm{core}} = 9 \times 0.02$ mJy ≈ 0.2 mJy. This is close to the reported upper limit and therefore more sensitive high-resolution observations should be able to detect the emission from the core.

However, an alternative explanation could be that the radio emission at 6 cm is not dominated by a stationary self-absorbed component but by a moving, relativistically beamed one. In such a case the lack of a radio core is simply due to the fact that the radiation is beamed away from us.

Finally we have to examine the possibility that the large scale (up to $\approx 21"$) is not of AGN origin but it is due mainly to star formation. If star-forming activity is co-extensive with the

observed radio emission then it would naturally explain its diffuse morphology. However, this is not very likely because the outer colors of the host galaxy are consistent with an old stellar population and there is no morphological or color evidence of a young stellar population at radii greater than 9 kpc (Hutchings & Neff 1991). A more likely scenario is that star formation occurs in a region more confined (<5 kpc) to the nucleus of $1821+643$. Indeed, most *IRAS* bright galaxies (like $1821+643$) have their main starbursts strongly confined in the nuclear region ($\lesssim 1$–3 kpc), and if this is the case for $1821+643$ then the observed large-scale radio emission could be due to a nuclear outflow powered by a central starburst. Such an outflow could be related to both AGN activity (since we know that there is an AGN there) and nuclear star formation since the phenomena are not mutually exclusive and are found coexisting in many bright *IRAS* galaxies (Edelson & Rieke 1987). In this scenario the large amount of dust/gas inferred by the FIR luminosity is the "fuel" for both the AGN and star formation.

6. CONCLUSIONS

We conducted high-sensitivity VLA observations in a sample of 12 RQQs selected for their strong FIR fluxes and/or indications of extended radio emission. We have found clear evidence for extended emission in four objects and we have successfully mapped it in the case of QSO $1821+643$. In three of these objects the emitted radio power is more than what is expected from their FIR luminosities and the FIR-radio correlation. This may indicate an AGN as well as star formation are powering the observed radio emission. In the case of $1821+643$ we have detected low brightness emission extending almost across the whole extent of the host cD galaxy and a linear feature (diffused jet?) aligned with a similar feature seen in previous high-resolution images. The origin of the observed low brightness extended component is not yet clear and star formation and/or the AGN may be responsible. However, the relative contributions of AGN and star formation in the large (21″) as well as in the small (<2″) scale need to be determined by further observations.

Millimeter CO observations are needed to estimate the molecular gas content of this galaxy and thereby verify the thermal (heated dust) origin of the observed FIR luminosity. Spectral index studies in the radio continuum would also be useful in order to see if there are any spectral index gradients from the QSO's center outward, indicating a nuclear outflow. Finally, high-sensitivity ($\lesssim 0.2$ mJy beam^{-1}) and high-resolution ($\lesssim 0\farcs4$) VLA observations are needed to search for an AGN-driven emission in the central 1–2 kpc of the nucleus by clearly establishing the presence of a one-sided jet and an associated core.

We would like to thank Dr. R. J. Ivison for his help and useful comments. We also acknowledge the support of an operating grant to E. R. S. from the Natural Sciences and Engineering Research Council of Canada. This research has made use of the NASA/IPAC Extragalactic Database (NED) which is operated by the Jet Propulsion Laboratory, Caltech, under contract with the National Aeronautics and Space Administration.

REFERENCES

Alloin, D., Gordon, M. A., & Antonucci, R. 1992, A&A, 265, 429
Baars, J. M., Genzel, R., Pauling-Toth, I. I. K., & Witzel, A. 1977, A&A, 61, 99
Barvainis, R. 1990, ApJ, 353, 419
Blandford, R. D., & Rees, M. J. 1991, in AIP Conf. Ser., Vol. 254, Testing the AGN paradigm, ed. S. S. Holt, S. G. Neff, C. M. Urry (New York: AIP), 12
Condon, J., & Broderick, J. 1988, AJ, 96, 30
de Grijp, M. H. K., Miley, G. K., & Lub, J. 1987, A&AS, 70, 95
Edelson, R. A., & Malkan, M. A. 1986, ApJ, 308, 59
Edelson, R. A., & Rieke, G. H. 1987, ApJ, 321, 233
Ellingson, E., Yee, H. K. C., & Green, R. F. 1991, ApJ, 371, 49
Helou, G., Soifer, B. T., & Rowan-Robinson, M. 1985, ApJ, 298, L7
Hughes, D. H., Robson, E. I., Dunlop, J. S., & Gear, W. K. 1993, MNRAS, 263, 607
Hutchings, J. B., & Neff, S. G. 1991, AJ, 101, 2001
Hutchings, J. B., Neff, S. G., & Gower, A. C. 1992, PASP, 104, 62
Kellermann, K. I., Sramek, R., Schmidt, M., Shaffer, D. B., & Green, R. 1989, AJ, 98, 1195
Kundt, W. 1987, in NATO ASI Ser., Vol. 208, Astrophysical Jets and Their Engines, ed. Wolfgang Kundt (Erice: NATO), 25
Kolman, M., Halpern, J. P., Shrader, R. C., Fillipenko, V. A. 1991, ApJ, 373, 57
Lacy, M., Rawlings, S., & Hill, G. J. 1992, MNRAS, 258, 828
Marscher, A. P. 1991, in AIP Conf. Ser., Vol. 254, Testing the AGN paradigm, eds. S. S. Holt, S. G. Neff, & C. M. Urry (New York: AIP), 377
Moffet, A. T. 1975, in Stars and Stellar Systems, Vol. IX, Galaxies and the Universe, ed. A. Sandage, M. Sandage, & J. Kristian (Chicago: Univ. of Chicago Press), 221
Morgan, W. W., & Dreiser, R. D. 1983, ApJ, 269, 438
Neugebauer, G., Miley, G. K., Soifer, B. T., & Clegg, P. E. 1986, ApJ, 308, 815
Preuss, E., & Fosbury, R. A. E. 1983, MNRAS, 204, 783
Schwab, F. R. 1980, Proc. SPIE, Adaptive Calibration of Radio Interferometer Data, 231, 18
Shakura, N. I., & Sunyaev, R. A. 1973, A&A, 24, 337
Telesco, C. M., & Drecher, R. 1988, ApJ, 334, 573
van der Kruit, P. C. 1973, A&A, 29, 263
Wrobel, J. M., & Heeschen, D. S. 1988, ApJ, 335, 677
Wunderlich, E., Klein, U., & Wielebinski, R. 1987, A&AS, 69, 487